Cement and Concrete Composites 145 (2024) 105313

Contents lists available at ScienceDirect

Cement and Concrete Composites

journal homepage: www.elsevier.com/locate/cemconcomp

Investigating PCM encapsulated NaOH additive for set-on-demand in 3D concrete printing

Sasitharan Kanagasuntharam [a], Sayanthan Ramakrishnan [a,b,*], Jay Sanjayan [a]

[a] Centre for Sustainable Infrastructure and Digital Construction, School of Engineering, Swinburne University of Technology, Hawthorn, Australia
[b] Centre for Future Materials, School of Engineering, University of Southern Queensland, Springfield, QLD, 4300, Australia

ARTICLE INFO

Keywords:
Concrete 3D printing
Stiffening control
Phase change material
Buildability
Set-on-demand
Thermal intervention

ABSTRACT

This study investigates the print head activation of an encapsulated additive to attain on-demand setting in 3D concrete printing for buildability enhancement. Sodium hydroxide (NaOH) is considered as a set accelerating additive, and it is encapsulated using a phase change material (PCM). The encapsulated NaOH is added during the initial mixing stage and the mix is heated at the print head to release the NaOH, which subsequently reacts with cementitious materials to attain the on-demand setting of the printed layer. The dosage of NaOH was varied from 0 to 5 wt% of the cement to determine the optimum dosage for buildability enhancement. The results showed that the static yield strength of the printable concrete after the print head activation increased with the NaOH dosage, however, this has resulted in reducing the compressive strength of the mixes. The fresh and hardened properties of the mixes with encapsulated NaOH were compared with the mix with nano-clay to assess two buildability enhancement approaches (set-on-demand vs traditional). It was found that the buildability enhancement using nano-clay was limited by pumpability constraints, whereas the activation of encapsulated NaOH was limited by compressive strength reductions.

1. Introduction

In the era of construction automation, extrusion-based 3D concrete printing (3DCP) has gained enormous attention for its various benefits, such as high productivity, safety, sustainability, and feasibility [1,2]. 3DCP is a formwork-free construction method where the fresh concrete is deposited layer by layer until the designed structure is built. Due to the absence of formwork, the deposited layers should exhibit high static yield strength (SYS) and viscosity to retain the shape of printed layers and to sustain the weight of subsequently stacked layers during printing. If the concrete has insufficient early age strength properties, the printed structure will collapse, resulting in buildability failure. Buildability failure in 3DCP can occur due to plastic collapse, elastic buckling or a combination of both [3]. The plastic collapse in 3DCP is governed by the static yield strength of the mix, whereas the elastic buckling is governed by the stiffness of the printed layer. As the early age SYS of the mix is proportional to its stiffness, the buildability of a mix can be enhanced by increasing the mix's SYS [4].

The enhancement of SYS and viscosity is usually achieved by adding thixotropic additives during the initial mixing stage [5,6]. However, thixotropic additives will also increase the SYS of the fresh concrete during the mixing and pumping stages, thus reducing the mix's pumpability. The pumpability of the mix is defined as the ease of transporting the mix to the print head. Therefore, a 3D printable mix needs to exhibit contradictory rheological behaviour during pumping and placement. More precisely, the mix should exhibit low viscosity and yield strength during pumping followed by high viscosity and yield strength during the placement. This was best achieved in previous studies by using chemical admixtures such as retarders and accelerators [7–11]. The retarders increase the open time of the mix by delaying the hydration reaction processes. However, once the mix reaches the print head, a precise dosage of the accelerator is injected to accelerate the hydration reaction which in turn increases the SYS development of the mix. A secondary mixing is required at the print head to mix the base mix and accelerators. This mixing is crucial for uniform mixing of accelerators and base mix and the mixing can only be conducted for a short duration due to the limited residence time constrained by in-line mixing chambers. Low mixing efficiency will result in non-uniform distribution of the accelerator, which can be detrimental to the hardened properties and durability of the printed structures. The long duration mixing can be achieved by designing a large print head mixer that will increase the residence time of mixing and hence, the mixing efficiency. However, such large print

* Corresponding author. Centre for Future Materials, School of Engineering, University of Southern Queensland, Springfield, QLD, 4300, Australia.
E-mail address: saya.ramakrishnan@usq.edu.au (S. Ramakrishnan).

https://doi.org/10.1016/j.cemconcomp.2023.105313
Received 13 July 2023; Received in revised form 19 September 2023; Accepted 3 October 2023
Available online 15 October 2023

heads would be heavy, bulky and limit the printing capability of intricate structures due to the interference of the print head with the previously printed layers. On the other hand, if the accelerators are mixed during the initial mixing stage, where the print head mixing is not required, the accelerators can be uniformly distributed within the mix. However, introducing the accelerators during the initial mixing stage can significantly reduce the pumpability and also the possible setting of concrete in pumping pipes or pumps that could lead to significant damage to the pumps [7].

To overcome the challenges associated with the accelerator mixing efficiency, Bhattacherjee et al. [7] proposed a post-processing method by spraying an accelerator on the printed layer to enhance the buildability of the mix. This eliminates the usage of secondary mixers, hence the challenges related to mixing efficiency. In addition, the spraying accelerator requires a less complicated print head, making the technology easier to implement in large-scale construction. However, spraying the accelerator only hardens the surface of the printed layer and the core of the layer remains soft. In contrast, the printed layer should exhibit a strong core for enhanced buildability and a soft/-malleable surface for better interlayer adhesion [12,13].

Another method to introduce the accelerators for 3DCP is to introduce encapsulated accelerators at the initial mixing followed by on-demand release to introduce the accelerator just after printing. This method will provide rapid SYS development after the release of accelerators without significantly affecting the flowability of the mixes prior to the accelerator release [8]. Moreover, this method eliminates the need for a secondary mixer and the associated limitations with the mixing efficiency. In a study [8], authors attempted to use gelatine capsules filled with liquid accelerators and subsequently, the accelerators were released by applying heat at the print head to dissolve gelatine capsules and to attain enhanced buildability. The heat was applied using IR lamps, but other sources of heat such as water bath and microwave can also be applied [14,15].

Encapsulation of the additives and their controlled release on an on-demand basis has been widely used in the medical and food industry [16,17]. For instance, the encapsulation technique is used for efficient drug delivery in the medical industry. Inspired by the outcomes, researchers investigated the encapsulation of phase change material (PCM) and other functional additives for the self-healing of concrete in building applications [18–20]. In addition, some previous studies have incorporated encapsulated accelerators and retarders to control the hydration of the cementitious mixes [21,22]. The encapsulated admixtures were then added to the cementitious mix to control its setting rate. The setting rate was controlled by applying heat, which melted the PCM shell to release the admixtures at the desired rate.

The concept of controlled release of chemical admixtures using an encapsulation technique was also investigated for 3DCP [8,15]. Here, Shao et al. [15] and Ramakrishnan et al. [8] used the polyethylene glycol and gelatine as encapsulation material respectively. In addition, the former study used microwave technology to heat the mix at the print head and melt the polyethylene glycol for controlled release of the additives. As concrete contains dielectric components, the application of microwaves will heat the mix due to frictional loss. The heat increases the temperature of the mix and melts the shell of the capsule. Microwave heating is reported as an efficient heating method for concrete as it heats the concrete faster and uniformly than other methods [12,14,23]. Graphite powder (microwave absorbents) was also added with the additives to enhance the efficiency of microwave heating. This reduces the microwaving duration required to melt the capsule shell, which in turn reduces the residence time of the concrete in the print head (where the heat is applied). Fig. 1 explains the preparation of capsules filled with buildability enhancing additives (accelerator and VMA) and microwave absorbents (graphite powder). While the results reported by Shao et al. [15] are promising, the implementation of microwave heating at the print head for construction can be challenging due to workplace safety issues.

This study investigates a set-on-demand method by introducing NaOH as a buildability enhancing additive which is encapsulated using a thermo-responsive phase change material (PCM). The on-demand release of NaOH was performed by using a water bath at the print head, which is relatively safe and can provide uniform heating. Moreover, the amount of NaOH is critical to achieve the desired SYS development for printing. An excessive amount of NaOH could be detrimental to the hardened properties and durability of concrete. Therefore, the encapsulated NaOH additive was introduced at various dosages and the fresh and hardened properties of the printable mixes were studied. The buildability enhancement using encapsulated NaOH was also compared with the addition of thixotropic additive during the initial mixing stage (traditional approach) to juxtapose two buildability enhancement approaches.

2. Materials and methods

Ordinary Portland cement (OPC) was used as the binder in this study. The OPC (type general purpose (GP)) complies with the standard AS3972 [24]. Two grades of sand, denoted as coarse sand (CS) and

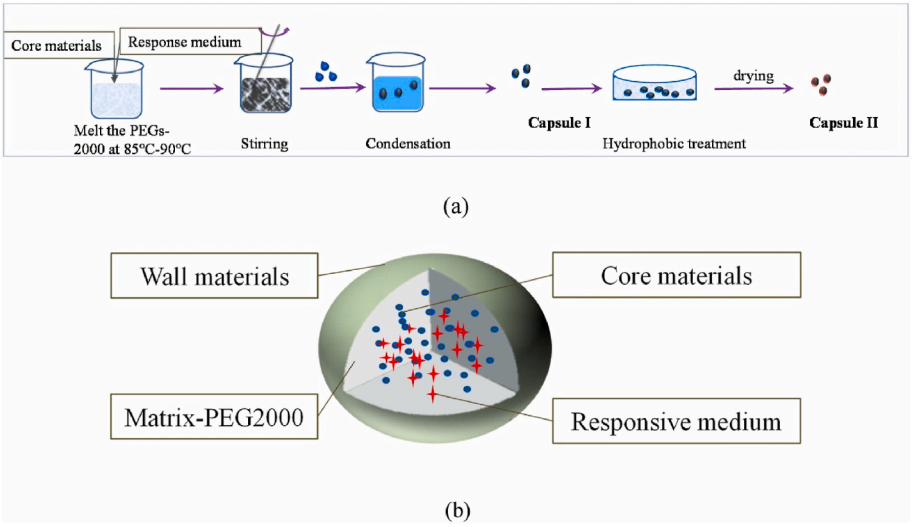

Fig. 1. (a) Steps involved in the preparation of capsules used in Ref. [15]. (b) Illustration of a capsule containing various additives required for the set-on-demand approach. The figure was taken from Ref. [15] with permission.

medium sand (MS), were supplied by Holcim, Australia. Chemical admixtures such as polycarboxylic ether-based superplasticiser (SP, MasterGlenium SKY 8379) and retarder (MasterSet RT 122) were used to enhance the workability and open time of the mix respectively. Sodium hydroxide (NaOH) pellets with a purity of 99% were supplied by Redox Pty. Ltd., Australia. In this study, NaOH was used as the set accelerator to enhance the buildability of the mix. The NaOH pellets were encapsulated using a thermo-responsive paraffin based PCM - RT31 from RUBITHERM®. The phase transition temperature of RT31 is about 31 °C. This study also compares the buildability enhancement achieved using the proposed set on demand approach (print head heating of mix containing encapsulated NaOH) with the traditional approach, where thixotropic additives are added during the initial mixing stage. Nano clay (also referred to as Magnesium Alumino Silicate - MAS) supplied by Active Minerals International, LLC was used as the thixotropic additive. The details of the nano clay used can be found in Ref. [25].

2.1. Encapsulation of NaOH

Fig. 2 shows the step-by-step procedure to prepare NaOH encapsulation. Firstly, the PCM was melted at 35 °C using a hot plate with temperature control. Once the PCM was melted to a clear liquid form, 240 g of NaOH was added to every 100g of PCM and mixed for 1 min to achieve a uniform distribution of NaOH. Subsequently, the NaOH and PCM blend was poured into cylindrical moulds of 5 mm diameter and 5 mm height. The mould filled with the mix was then transferred to a climate controlled thermal chamber operated at 15 °C. After cooling for 10 min, the encapsulated NaOH was demoulded and coated with another thin layer of PCM by dipping the capsules into the molten PCM. Finally, the double coated NaOH was placed in the thermal chamber operated at 15 °C for 60 min to solify the shell of the capsules.

2.2. Preparation of printable concrete

The mix design of materials used in this study is given in Table 1. Here, two buildability enhancement strategies were investigated: 1) Print head heating of the mix with encapsulated NaOH to attain on-demand enhancement in buildability. 2) Adding thixotropic additives (nano clay) during the initial mixing stage. The mix M – P represents the second buildability enhancement strategy, whereas the rest of the mixes represent the first buildability enhancement strategy. Here, the encapsulated NaOH was added at dosages varying from 0 wt% to 5 wt% of cement to the mix. The suffixes “H” and “M” denoted the print head heating and print head mixing. For instance, the mix M-2.5, M-2.5H and M-2.5HM refers to the mix with 2.5% of encapsulated NaOH without printhead heating and mixing, with printhead heating only and with simultaneous printhead heating and mixing respectively. In addition, the mixes denoted with M-2.5HM-0W and M-5HM-0W represent the printable mixes with direct addition of NaOH without encapsulation at 2.5% and 5% respectively. These samples were prepared to distinguish the effect of NaOH and PCM on the compressive strength of concrete as discussed in Section 4.2.1.

The ratio between cement and sand was kept constant at 1.5 for all the mixes. Similarly, the superplasticiser and retarder dosages were also kept constant at 4.71 g/kg and 5 g/kg of OPC respectively for all the mixes. In mixes M-2.5 and M – 5, the NaOH dosage was varied from 2.5 wt% to 5 wt% to investigate the effect of NaOH dosage on the fresh and hardened properties of the printable mix. The dosage of nano clay in the mix M – P was chosen as 0.4 wt% following the preliminary study. Further addition of nano clay showed significant difficulty in pumping and extrusion processes.

The mixing process is as follows. Initially, the dry ingredients (cement and sand) were transferred to the mixing bowl and mixed at 61 rpm for 1 min. Simultaneously, a solution of water, superplasticiser (SP) and retarder was prepared according to the mix design shown in Table 1. After the dry mixing, the prepared solution was gradually added, and the mixing was conducted at 125 RPM for 2 min. After that, the wet mixing was paused, and the materials adhered to the sides and bottom of the mixing bowl and blades were scrapped to ensure homogenous mixing. Subsequently, the wet mixing was continued for 1 min at 61 RPM. The prepared capsules at a predefined dosage were then added to the wet cementitious mix and mixed for 30 s at 61 RPM for uniform distribution. Print head heating was simulated in the laboratory by exposing the blended cementitious mix with encapsulated NaOH to a water bath maintained at 60 °C. The mix was exposed to the heating for 30 s with and without simultaneous mixing according to the mix type. The heating process is expected to melt the encapsulation and release NaOH to enhance the buildability of the printed layer.

3. Experimental methodology

3.1. Static yield strength (SYS) evolution with time

A slow penetration test was employed to assess the SYS evolution of various printable mixes given in Table 1. The mix after print head activation (by heating or heating with mixing) was transferred to the

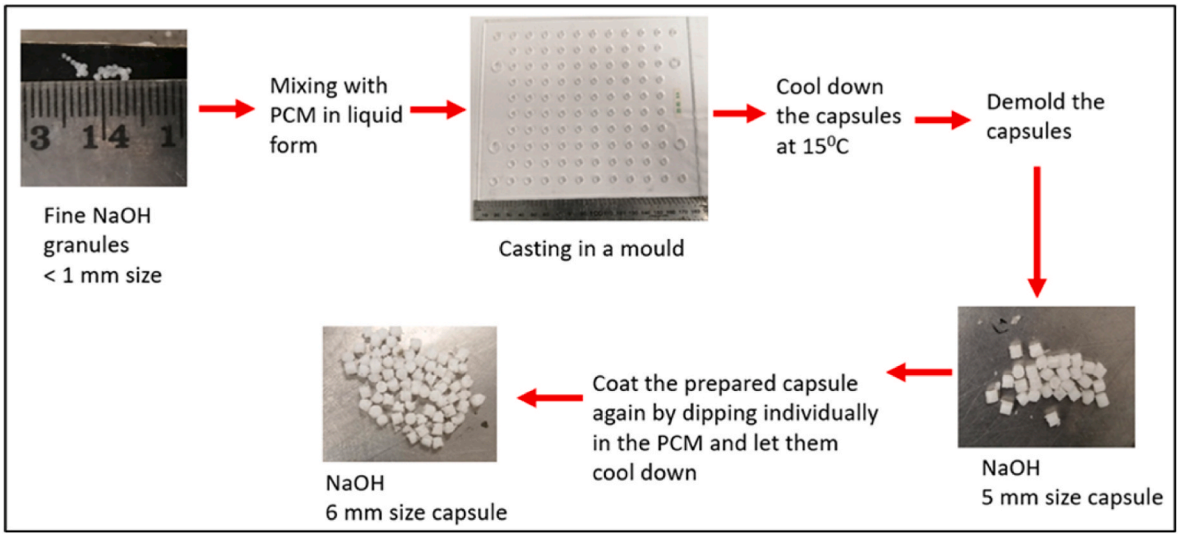

Fig. 2. Step by step NaOH encapsulation procedure.

Table 1
Mix design of the materials.

Mix ID	Cement (OPC)	Water/ Cement	Sand/Binder		WRA (g/kg of OPC)	Retarder (g/kg of OPC)	NaOH dosage (g/kg of OPC)	heat applied	Nano clay (g/kg of dry mix)	Mixing after heating
			Coarse	Fine						
M-P	1	0.33	1	0.5	4.71	5	0	N	4	N
M							0	N	N/A	N
M-2.5							25	N		N
M-5							50	N		N
M-2.5H							25	Y		N
M-5H							50	Y		N
M-2.5HM							25	Y		Y
M-5HM							50	Y		Y
M-2.5HM-0W							25 (without PCM)	Y		Y
M-5HM-0W							50 (without PCM)	Y		Y

sample cup with 80 mm diameter and 120 mm height. A conical needle as shown in Fig. 3 connected to a 500 N load cell was slowly penetrated into the fresh concrete. The penetration rate was controlled at 10 mm/h using the displacement controlled compression loading setup in a Mechanical Testing System (MTS) machine. The resistance of penetration was continuously measured by the load cell and was used to determine the SYS as per the method proposed in Refs. [26,27]:

$$\tau = \frac{F}{\pi R\sqrt{R^2 + h^2}} \quad \text{Equation 1}$$

where, F is the penetration resistance force measured by the load cell (N), R is the cone radius (mm), and h is the cone height (mm). The first measurement was conducted 5 min after mixing to allow sufficient time for sample preparation and experimental set up [28].

3.2. Elastic modulus of the printed layer

The buildability of the printable mix is governed by both SYS and the stiffness of the printed layer. The SYS and its evolution with time govern the plastic collapse failure, whereas the stiffness of the filament governs the elastic buckling failure during printing. Therefore, the stiffness was determined by measuring the elastic modulus of the printed layer at various rest times after printing (10–40 min). The experimental setup used to measure the elastic modulus of the printed layer is shown in Fig. 5. The fresh concrete after preparation was transferred to a customised 3D printer to print 200 mm long, 40 mm wide and 40 mm thick two-layered specimens. The customised 3D printer, as shown in Fig. 4, consists of a piston-type extruder connected to a cylindrical barrel with the capacity to hold 1.2 L of fresh concrete. The other side of the barrel was connected to a rectangular nozzle of 40 mm wide x 20 mm height to control the shape of the extruded filament.

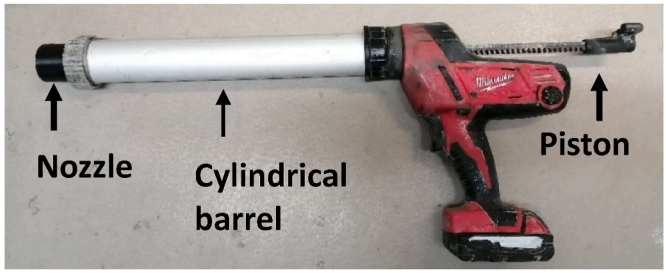

Fig. 4. A customised 3D printer consists of a piston-type extruder.

After printing, the specimens were kept at rest in a temperature and humidity-controlled environment until test. The printed specimens were vertically compressed at a displacement-controlled loading rate of 10 mm/min using the MTS machine. The applied load was measured using a 10 kN load cell attached to the machine. The generated load vs displacement data was converted to a stress vs strain graph and the slope of the linear portion of the graph (i.e., up to the 5% of strain) was used to determine the elastic modulus of the printed element. It is worth mentioning here that since the printed specimens were in the fresh state, they deformed axially during unconfined compression, thus the cross-sectional area under load changed continuously during the test. Therefore, a corrected cross-sectional area is required to convert the load vs displacement graph to the stress vs strain graph. However, as the elastic modulus was determined from the linear section up to the 5% strain limit, the changes in cross-sectional area while loading were insignificant in the measuring zone. Moreover, the results were used to compare the stiffness of various mixes, therefore, the error due to change in the

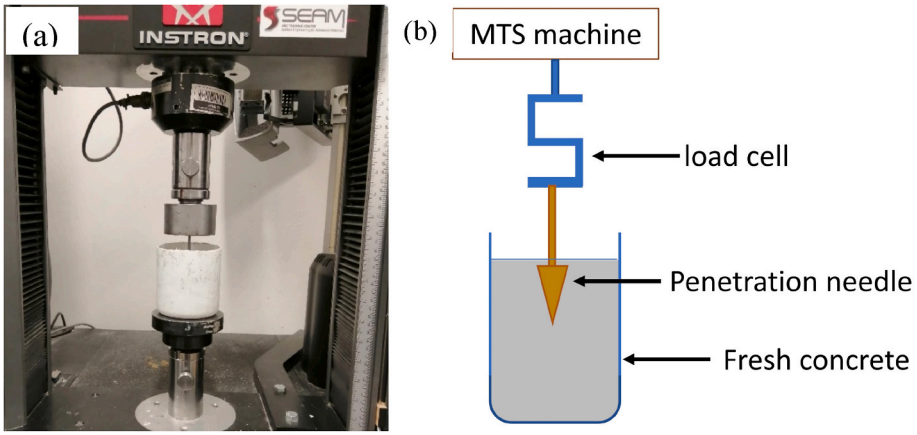

Fig. 3. (a) Experimental setup (b) schematic diagram of test setup used for determining the SYS development with time.

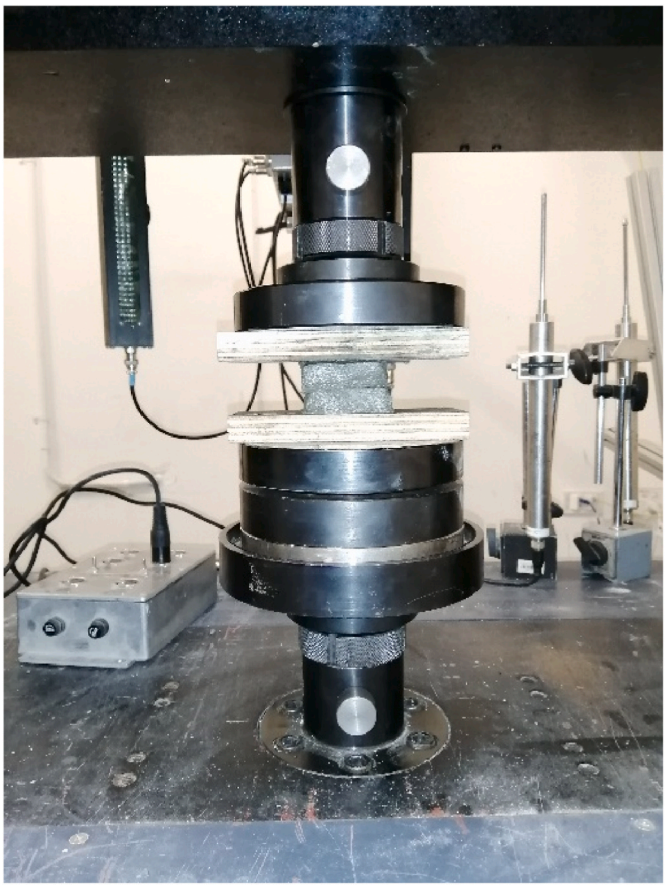

Fig. 5. Elastic modulus test of printed filament containing encapsulated NaOH.

cross-sectional area will remain the same for all specimens.

3.3. Mini-slump test

A mini slump test as per ASTM C1437 was performed for mixes shown in Table 1 to determine the pumpability properties prior to the print head activation [29]. As the mixes with encapsulated NaOH are heated at the print head, the mix should show good pumpability properties before heating. For this test, the mixes M, M-2.5 and M − 5 were transferred to a truncated mini-slump cone. The dimensions of the truncated cone are 70 mm (top radius), 100 mm (bottom radius) and 100 mm (Height). After filling the cone with the fresh mix, the cone was lifted to measure the spread diameter. Similarly, the spread was measured for various time intervals, ranging from 0 to 60 min from mixing. The variation in spread diameter with time was measured for the mix with nano clay to compare the pumpability of the proposed approach with the thixotropic additive based approach.

3.4. Mechanical properties of concrete containing encapsulated NaOH additives

While NaOH is known to accelerate the setting rate of the concrete, excessive addition of NaOH can be detrimental to the hardened properties. Moreover, the mix needs to exhibit sufficient hardened properties as it is developed for construction applications. Therefore, the mechanical properties of encapsulated NaOH additives incorporated concrete mixes were assessed by the compressive strength of mould cast and 3D printed specimens. For mould cast specimens, the mixes after print head activation were poured into 50 X 50 × 50 mm^3 stainless steel moulds and compacted using a mechanical vibrator. Following the mould-casting process, the moulds were sealed and cured at ambient conditions for 24 h. After 24 h of sealed curing, the specimens were demoulded and placed in the water bath until the test date. On the test date, the cubes were removed from the water bath and loaded under compression until failure. The loading rate was maintained at 0.33 kN/s for all the specimens. Three cubes for each mix design were tested for compressive strength and the average compressive strength along with one standard deviation was plotted.

On the other hand, the fresh printable mixes after print head activation were 3D printed to compare the compressive strength of 3D printed specimens with the mould cast specimens. Previous studies have reported that the printed specimens show anisotropic compressive strength properties [30–32]. Therefore, the compressive strength of the printed specimens was determined for three loading directions. i.e., longitudinal, lateral and perpendicular directions. A two layered prism of 200 mm long, 40 mm wide and 40 mm thick was printed using a customised 3D printer explained in section 3.2. After printing, the two-layered prisms were sealed and cured for 24 h followed by curing in the water bath until the test date. On the test date, the prisms were cut into 40 mm × 40 mm x 40 mm cubes to test the compressive strength. Three cubes for each mix design and loading direction were tested and the average value was reported with one standard deviation. The mix group with nanoclay additive was also tested for mould cast and 3DCP specimens to compare different buildability enhancement approaches.

3.5. Interlayer bond strength test

The interlayer bond strength test was conducted on the 40 x 40 × 40 mm^3 specimens extracted from two layered prisms of 200 mm × 40 mm x 20 mm (width) printed using the customised 3D printer. The experimental setup consists of metallic brackets that are connected to a universal MTS machine. The printed samples were supported with metallic brackets and loaded under tension until failure. A 4 mm triangular notch was created at both sides of the interlayer to ensure the failure plane at the interlayer. Moreover, the notch also assists in placing the samples onto the metallic brackets. The samples were tested in displacement control method at 0.5 mm/s. Three samples were tested for each group and the average interlayer bond strength was reported along with one standard deviation.

3.6. Apparent volume of permeable voids test

The apparent volume of permeable voids (AVPV) of the mixes with various NaOH dosages and nano clay was determined for mould cast and printed specimens. The AVPV test was conducted as per ASTM C642, and the void volumes were determined using Equation (2). In this test, initially, the oven dry weight (w1) of the specimens was measured by heating the specimen at 105 °C until a constant weight was reached. Then, the samples were immersed in boiling water for 5 h and the boiled surface dried mass was measured as w2. Finally, the samples were suspended in water using a metalling cage and the suspended weight was measured as w3. The AVPV was determined by following Equation (2). The average AVPV determined for three specimens was reported along with one standard deviation of the results.

$$AVPV = \frac{w2 - w1}{w2 - w3} \times 100\% \qquad \text{Equation 2}$$

4. Results and discussion

4.1. Early age properties of concrete containing additives

4.1.1. Slump flow

The effect of incorporating buildability enhancing additives on the pumpability of the printable mixes was determined by measuring the slump flow of the mixes before thermal activation. Three mixes were studied for pumpability test – mixes containing 2.5 wt% and 5 wt%

encapsulated NaOH and the mix containing nano clay as the buildability enhancing additive. In addition, the mixes containing encapsulated NaOH were also tested after thermal activation to assess their ability to produce zero slump mixes required for shape retention just after printing. Fig. 6 shows the slump flow measurements of various mixes at different rest times from mixing. As shown in Fig. 6, the mix with nano clay (M − P mix) showed a flow diameter of 100 mm, which indicates that the mix has zero slump flow shortly after mixing. While such properties are beneficial to enhance buildability, the mix would have poor pumpability. it is primarily due to the thixotropic properties of nanoclay in concrete, where electrostatic attraction exhibited by the nanoclay particles brings the cement particle together and forms large flocculants. These flocculants thicken the concrete and restrict the flow of concrete [33]. On the other hand, the mixes with encapsulated NaOH showed excellent pumpability. For instance, the mix with 2.5 wt% encapsulated NaOH exhibited a slump flow diameter of 185 mm shortly after mixing, which is 85% higher than the slump flow exhibited by the mix with nano clay. Similarly, the mix with 5 wt% encapsulated NaOH exhibited a slump flow diameter of 160 mm shortly after mixing, which is 60% higher than the slump flow exhibited by the mix with nano clay.

It is also interesting to note that the thermal activation of mixes with encapsulated NaOH (M-2.5HM and M-5HM) showed 100 mm flow diameter immediately after the heat activation (i.e., at 0 min), indicating that the zero-slump flow properties. The rapid transformation of mixes from high flowability to zero slump immediately after thermal activation is advantageous to meet the contradicting requirements of rheological properties in 3DCP. For instance, the mixes containing 2.5 wt% and 5 wt% of encapsulated NaOH showed a flow diameter of 185 mm and 160 mm respectively before thermal activation (M-2.5 M and M-5M). However, the corresponding mixes transform to 100 mm (zero slump by remaining in the shape of cone) immediately after mixing (M-2.5HM and M-5HM).

In addition, the slump flow was found to reduce with the increasing dosage of NaOH, even before the thermal activation. The slump flow shortly after mixing was reduced by 13.5% when the dosage of NaOH was increased from 2.5 wt% to 5 wt%. It could be due to the increment in the solid content of the mix. The increment in NaOH dosage increases the number of capsules added to the mix, which in return increases the solid content in the mix. For a specific water to binder ratio, an increment in solid content reduces the workability of the mix since the amount of free water to lubricate/wet the surface of solid particles is reduced. In addition, the capsules act like large aggregate (i.e. 6 mm size), which further reduces the slump flow of the mix at higher dosages [34,35]. Nevertheless, the reduction in slump flow with time was similar for different NaOH dosages of 2.5 wt% and 5 wt%. In the case of a mix containing 2.5 wt% of NaOH, the slump flow value was reduced from 185 mm to 150 mm (18%) after 45 min. Similarly, the slump flow value was reduced from 160 mm to 130 mm (18%) after 45 min for the mix containing 5 wt% of NaOH. This informs that the mixes with encapsulated NaOH represent better pumpability and long open time than the mix with nano-clay (M − P), while meeting the zero slump requirements just after the thermal activation.

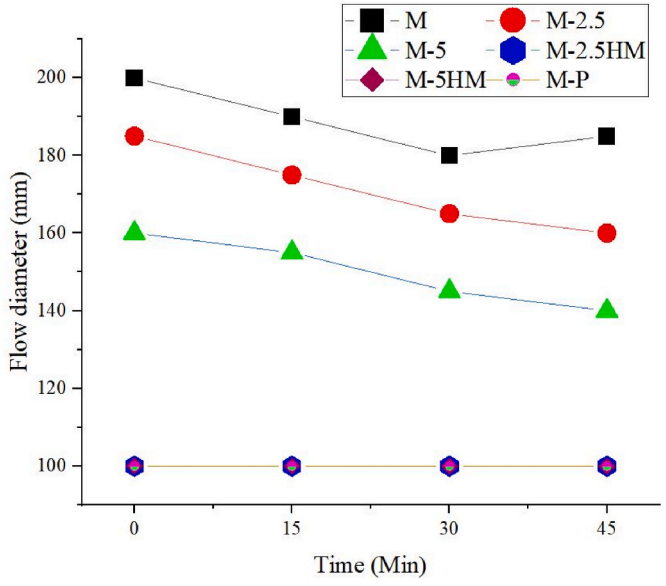

Fig. 6. Slump flow values of mixes with encapsulated NaOH at various dosages and nano clay as buildability enhancing additive.

4.1.2. *Static yield strength evolution with time*

The SYS development of various mixes with time, as measured from the slow penetration test, is depicted in Fig. 7. For this purpose, the mixes containing 2.5 wt% and 5 wt% of NaOH dosage were tested for the conditions of 1) before activation (M-2.5 and M − 5), 2) thermal activation only (M-2.5H and M − 5H) and thermal activation with simultaneous mixing (M-2.5HM and M-5HM) along with the control mix (M) and mix with nanoclay additive (M − P). It was found that after heating, the mix with 2.5 wt% and 5 wt% of NaOH exhibited SYS of 12.3 kPa and 33.8 kPa at 30 min which is approximately 3 times and 5.7 times higher than the same mixes without heating respectively. As NaOH is encapsulated using a thermo-responsive material (PCM), heating the mix melts the PCM and releases NaOH. Subsequently, the NaOH increases the alkalinity of the mix which in return accelerates the dissolution of sulphate ions and aluminate phases in cement. The dissolved sulphate ions and aluminate phases react with each other to form ettringite, increasing the SYS of the mix. The micromorphology characterisation of hardened 3D printed concrete specimens discussed in Section 4.21 indicates the formation of the ettringite (the needle-like structures) on the PCM residue in concrete.

An increment in NaOH dosage was found to increase the SYS development of the mix after heating. For instance, when the NaOH dosage was increased from 2.5 wt% to 5 wt%, the SYS at 30 min was increased by 174%. Interestingly, simultaneous mixing and heating further enhance the SYS development of the mix. Due to the large size of the capsules, the melting of PCM creates localised spots of concentrated NaOH in the mix even though the encapsulated NaOH was uniformly distributed during the initial mixing stage. Simultaneous mixing and heating could restrict the formation of such concentrated spots and disperse the released NaOH uniformly in the mix. This will result in the enhanced reaction between the NaOH and cement particles which in

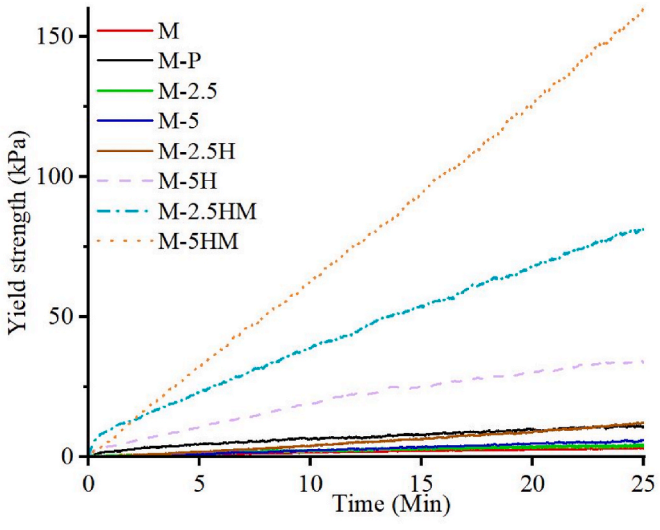

Fig. 7. Static yield strength development of mixes with encapsulated NaOH and nano clay.

turn accelerates the SYS development of the mix. At 2.5 wt% dosage, the fresh concrete after simultaneous heating and mixing exhibited a SYS of 81.6 kPa at 30 min, which is 3.3 times higher than the same mix after only heating. Similarly, the mix with 5 wt% dosages exhibited a SYS of 159 kPa at 30 min after simultaneous mixing and heating, which is 3.7 times higher than the same mix after only heating. It is also interesting to note that the SYS determined for the mix with 2.5 wt% NaOH after simultaneous heating and mixing (M-2.5HM) was 141% greater than the mix containing 5 wt% of NaOH with heating only. This suggests that the simultaneous heating and mixing will provide high SYS development at low NaOH dosage, compared to heating only even at higher dosages.

The buildability enhancement of the proposed encapsulated NaOH method was also compared with the most commonly studied buildability enhancement method - by adding nano clay in the initial mixing stage (M − P mix). The addition of nano clay increased the SYS development of the mix with time. For instance, the mix with nano clay showed 9 times higher SYS than the control mix at 30 min. In addition, the nano clay mix showed similar SYS development to the mix with 2.5 wt% NaOH dosage that was only heated at the print head. However, with simultaneous mixing and heating, the mix with 2.5 wt% NaOH exhibited a significantly faster SYS development rate than the mix with nano clay. On the other hand, increasing the dosage of NaOH showed a much higher SYS development rate than the mix with nano clay.

4.1.3. Elastic modulus development of the printed layers

The stiffness of the mixes with the encapsulated NaOH activation process was assessed for various time intervals (i.e., from 10 to 40 min) by determining the elastic modulus of the printed filaments after thermal activation. It was concluded from the previous section that to attain maximum buildability, the mix with encapsulated NaOH needs to be simultaneously mixed and heated at the print head. Therefore, the elastic modulus was determined for mixes following heating and mixing processes and the mixes activated at the print head by heating only process was not considered. Fig. 8 shows the elastic modulus of the printed specimens for the mixes of M − P, M-2.5HM and M-5HM at various time intervals from 10 to 40 min. The elastic modulus development with time suggests that irrespective of the mix type, the elastic modulus of the printed specimens increases with time. This is due to the thixotropic behaviour of concrete as well as the hydration of cement with time.

The comparison of elastic modulus development between different mix groups reveals that the M-2.5HM and M-5HM mixes showing rapid elastic modulus development than M − P mix. For instance, the elastic modulus of the M − P mix increased from 484 kPa to 916 kPa when the rest time increased from 10 to 40 min whereas, the M-2.5HM and M-5HM mixes showed an increment from 2215 kPa to 3513 kPa and 3039 kPa–5989 kPa respectively. This demonstrates the significantly higher initial elastic modulus and its growth with time for encapsulated accelerator incorporated mixes, compared to the mix containing the nanoclay additive. It is also noted that the evolution of elastic modulus with time follows a similar trend as that of SYS evolution with time. This implies that the proposed buildability enhancement approach by using the encapsulated NaOH activation method increases both the SYS and stiffness of the mix after activation.

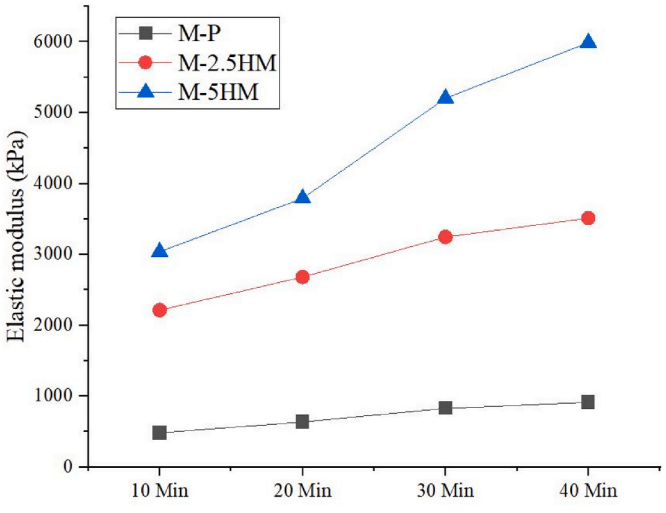

Fig. 8. Evolution of elastic modulus with time for mixes with varying encapsulated NaOH dosage (2.5 wt% and 5 wt%) and nano clay.

The SYS and stiffness evolution with time were compared according to Equation (3) [27]. As the SYS was only determined up to 25 min, the SYS and elastic modulus data corresponding to 10 min and 20 min were used for the comparative assessment.

$$\frac{E_{Co}(t)}{E_{co}(t+i)} = \left(\frac{f_c(t)}{f_c(t+i)}\right)^n \quad \text{Equation 3}$$

Where, E_{co} (t) = elastic modulus at a given time 't'; E_{co} (t + i) = elastic modulus after 'i' min from earlier measurement; fc (t) = SYS of the concrete at a given time 't'; f_c (t + i) = SYS of the concrete after 'i' min from earlier measurement, n = constant parameter.

The measured SYS and elastic modulus for various mixes are given in Table 2. As can be seen from the Table, the initial elastic modulus was determined to be higher than the initial SYS for all mixes. However, the stiffness growth rate was slower than the SYS growth rate of the mixes with encapsulated NaOH (Mixes M-2.5HM and M-5HM). A similar trend was also observed in other set-on-demand mixes introduced for concrete 3D printing applications [27]. Meanwhile, in the case of the mix with nanoclay (Mix M − P), the stiffness growth rate was equivalent to the SYS growth rate. A similar observation was made with traditional mixes for concrete 3D printing applications by Wolf et al. [36]:

According to Breitenbucher et al. [37], the 'n' value of around 0.33 represents the concrete after setting. Usually, for traditional printable mixes, the 'n' value was determined to be around 1 [36]. Therefore, it is justifiable to categorise mixes M-2.5HM and M-5HM as set-on-demand printable mixes (Table 2). It is worth mentioning here that the parameter 'n' will vary its value with respect to the mix's age. However, it is most likely that the SYS growth rate to always remain higher than the stiffness growth rate for set-on-demand mixes [27].

4.2. Hardened properties

4.2.1. Compressive strength

The compressive strength of various printable mixes at 7 and 28-day age are shown in Fig. 9. It is worth mentioning here that the mixes with encapsulated NaOH were simultaneously heated and mixed before casting to uniformly disperse the released NaOH into the mix. As one can observe in Fig. 9, the M − P mix showed increased compressive strength at 7 and 28-day strength, compared to the control specimen (Mix M). This is attributable to the fact that nano clay brings cement particles together through electrostatic interactions as well as fills the pore and provides nucleation sites for hydration reactions [25,38]. Therefore, the addition of nanoclay increases the strength of hardened concrete. The 7 and 28-day compressive strength of M − P mix was increased by 17.8%

Table 2
Relationship between the buildability parameters for different mixes.

Mix ID	Time (Min)	Stiffness (kPa)	Static yield strength (kPa)	n
M-P	10	484	6.48	0.76
	20	638	9.33	
M-2.5HM	10	2215	38.92	0.34
	20	2682	68.53	
M-5HM	10	3039	62.38	0.31
	20	3793	126.09	

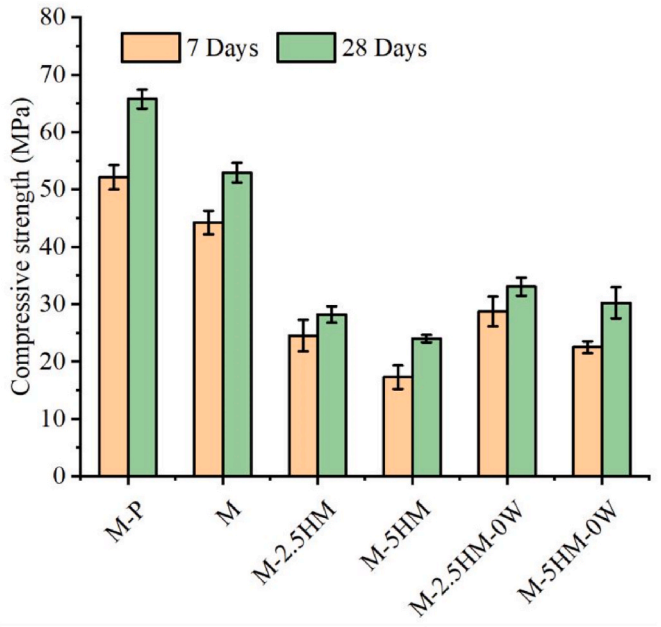

Fig. 9. 7- and 28-day compressive strength of mould cast specimens with, without encapsulated NaOH and nano clay (error bar represents mean ± one standard deviation).

and 24.1% respectively, compared to the control mix (mix M). Meanwhile, the compressive strength properties were reduced with the addition of encapsulated NaOH. It was also determined that the reduction in the compressive strength increased with the increment in the NaOH dosage. For instance, the 7-day compressive strength was reduced from 44.3 MPa to 24.5 MPa (44.6% reduction) with the addition of NaOH at 2.5 wt% dosage. Moreover, when the dosage was increased from 2.5 wt% to 5 wt%, the compressive strength was further reduced by 29.3%. The corresponding changes in 28-day compressive strength were determined as 47% at 2.5 wt% dosage with a further reduction of 14.9% when the dosage was increased from 2.5 wt% to 5 wt%.

The reduction in compressive strength properties with the introduction of NaOH accelerator can be explained as follows. When the NaOH is released during the activation (i.e., heating and mixing process), the alkalinity of the concrete is increased and hence, the dissolution of sulphate ions and aluminate phases in cement is accelerated. The dissolved components of cement then react to form a hydrated calcium aluminium sulphate hydroxide phase, known as ettringite. The excessive formation of ettringite deprives sulphate ions in the mix. Sulphate depletion further enhances the hydration of C_3A and impedes the hydration of C_2S and C_3S present in the cement. As the hydration product of C_3A is less stable than C_2S and C_3S products, the hardened properties of the concrete are significantly reduced with the addition of NaOH [39,40]. On the other hand, the reduction in compressive strength can also be attributed to the presence of residual PCM after activation.

To distinguish the effect of these two scenarios on the compressive strength of concrete, two mixes of M-2.5HM-0W and M-5HM-0W were prepared, where 2.5 wt% and 5 wt% NaOH were directly added to the mix without the PCM encapsulation. This will eliminate the effect of residual PCM in concrete. The compressive strength of these specimens is also included in Fig. 9. As can be seen from Fig. 9, the 7 and 28-day compressive strength of mixes with the direct addition of NaOH also significantly reduced. For instance, the direct incorporation of NaOH at 5% (mix M-5HM) showed a strength reduction of 49.1% and 42.7% at 7 and 28 days, compared to the control specimen. Meanwhile, the encapsulated NaOH at 5% (mix M-5HM-0W) showed corresponding strength reductions of 61.1% and 54.4% respectively. From this comparison, it can be concluded that the major proportion of strength loss in this method is caused by the NaOH additive, which is primarily due to the formation of secondary ettringite. The further reduction is attributed to the PCM that reduces the matrix strength of concrete. Past studies have reported that the incorporation of PCM into concrete would reduce the compressive strength [41,42].

The micromorphology of M, M-2.5HM and Mix M-5HM mixes after 28 days of age are investigated to understand the morphology of NaOH,

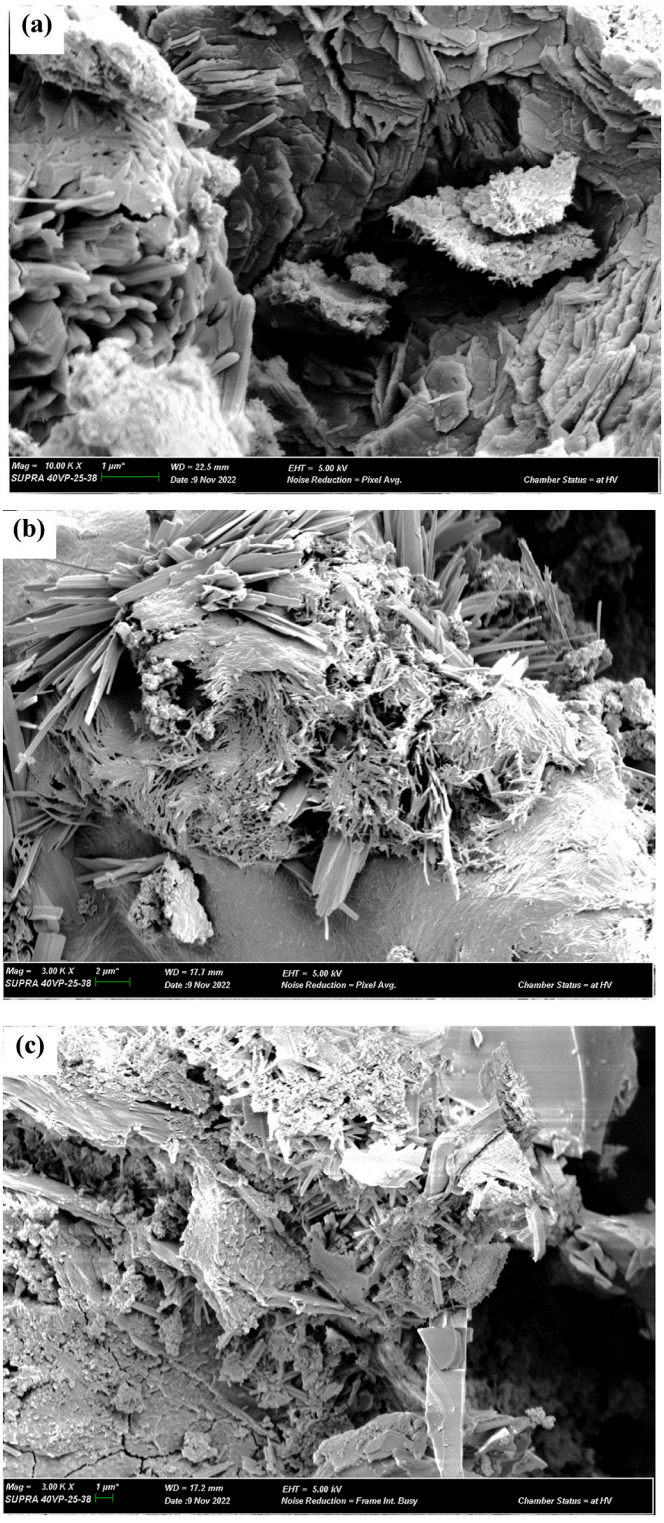

Fig. 10. SEM images of (a) Mix M, (b) Mix M-2.5HM and (c) Mix M-5HM after 28 days of age showcasing the formation of ettringite.

PCM and hydration products of the proposed encapsulated NaOH activation method. The SEM images of these specimen groups are shown in Fig. 10. From Fig. 10, it is evident that the formation of ettringite on the PCM surface for the mixes of M-2.5HM and M-5HM. This reveals that the PCM shell melts and releases the encapsulated NaOH during the activation process. Following the activation process, the ettringite is rapidly formed in these mixes as seen from the SEM images. Meanwhile, the SEM image of the control specimen indicates that there are no ettringite formed. Therefore, the accelerated ettringite formation in the encapsulated NaOH incorporated mixes restricts the formation of the calcium silicate hydrate (C–S–H) network as discussed earlier, leading to low hardened properties. Despite the reduction in compressive strength of the proposed encapsulated NaOH activation method, the mixes with 2.5% NaOH dosage showed compressive strength above 25 MPa, which is sufficient for most construction applications [43]. Therefore, the proposed set-on-demand method presents as a viable technology for construction applications. However, future studies are required to further investigate the effect of NaOH additives on the long-term mechanical and durability properties of printable concrete.

On the other hand, the compressive strength properties of 3D printed specimens for various mix groups are depicted in Fig. 11. The compressive strength varies with the loading direction for all the mixes, showcasing an anisotropic behaviour similar to previous studies [30, 44]. For all mix groups, the compressive strength was highest in the perpendicular direction and the lowest in the lateral direction. A similar relationship between the compressive strength and the loading direction was also found in Ref. [45]. This is attributable to the fact that the longitudinal and lateral directional strengths are interfered by the weak interlayer, thus causing the weak compressive strength. For the perpendicular strength test, the weak interlayer plane is perpendicular to the loading direction leading to the highest strength properties.

Apart from the anisotropic strength behaviour, it is also observed that the introduction of encapsulated NaOH reduces the compressive strength of 3D printed specimens in all directions. For instance, the 28-day compressive strength at the perpendicular direction was reduced by 51% and 57% for the mixes with 2.5 wt% and 5 wt% of NaOH, compared to M − P mix. The corresponding reduction in the longitudinal direction was determined as 43% and 55% respectively at 28 days. The 3D printed specimens showed a reasonable agreement of the strength reduction compared to mould cast specimens, suggesting that this is primarily governed by rapid early age ettringite formation in these mixes.

It is also interesting to note that the printed specimens exhibited lower compressive strength than the mould cast specimens for all loading directions. For instance, the 28 days longitudinal compressive strength of printed specimens of M-2.5HM, M-5HM and M − P mixes were reduced by 35.5%, 60.6% and 68.2%, compared to mould cast specimens. The corresponding strength reduction in lateral direction was determined as 42.8%, 65.6%, and 75.4% respectively. The perpendicular loading direction showed slightly less strength reduction of 25.4%, 23.4% and 34.2% for M-2.5HM, M-5HM and M − P respectively. The reduction in compressive strength of 3D printed specimens, compared to mould-cast specimens, could be due to the increased interlayer and intralayer porosity of 3D printed specimens as reported previously [46]. Due to these process-induced defects, the mix M-5HM exhibited 28-day compressive strength below 15 MPa for 3D printed specimens. Such low strength of concrete will hinder many structural concrete applications. Our future studies will investigate the methods to overcome significant strength losses in the 3DCP method, particularly for the stimuli-responsive method using the encapsulated additives.

4.2.2. 7- and 28-day interlayer bond strength

The interlayer bond strength of the printed specimen is primarily governed by the malleability and the surface moisture content of the printed layers [47]. The high SYS of printed layers would lead to low malleability, resulting in a reduced contact area between the stacked layers and hence showing the weak interlayer bond strength. Therefore, the effect of NaOH dosage on the 7- and 28-days interlayer bond strength was studied and compared with the nanoclay incorporated mix as shown in Fig. 12. As can be seen in Fig. 12, among all mixes, the nanoclay addition showed the highest interlayer bond strength than the NaOH activated mixes. For instance, the interlayer bond strength of M − P mix at 7 and 28 days were 1.16 MPa and 1.31 MPa respectively, which is 63.3% and 67.9% higher than the interlayer bond strength obtained for 2.5 wt% NaOH and 94.8% and 87.1% higher than the 5 wt% NaOH

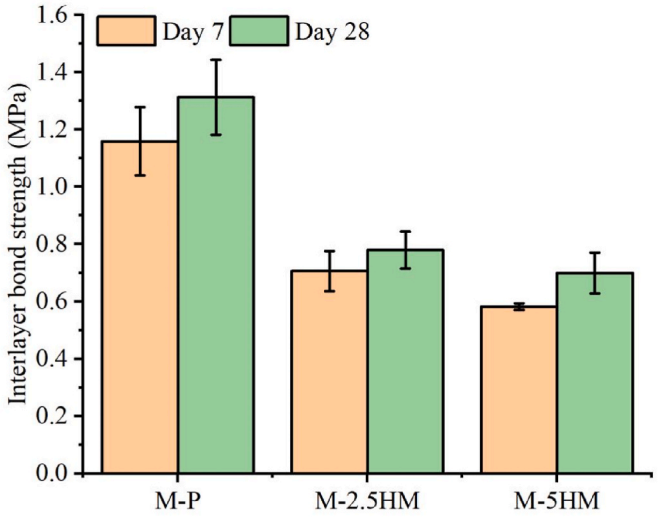

Fig. 12. 7- and 28-day interlayer bond strength of the specimens printed using mixes containing encapsulated NaOH at various dosages and nano clay (error bar represents mean ± one standard deviation).

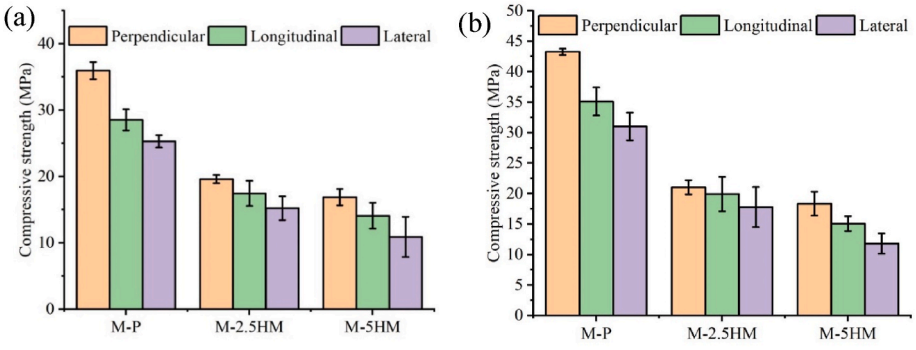

Fig. 11. (a) 7 and (b) 28-day compressive strength of the printed specimens with encapsulated NaOH and nano clay at three loading directions (error bar represents mean ± one standard deviation).

dosage mix. This could be due to the rapid hardening of the printed layer for the mixes M-2.5HM and M-5HM, thus reducing the malleability of printed layers and creating a porous interlayer while stacking (cold joints). Meanwhile, the low interlayer bond strength of mixes with NaOH can also be associated with the reduced matrix strength of these specimens as observed from the compressive strength results.

Therefore, to understand the attributable reason governing the low interlayer bond strength of the printed specimens with encapsulated NaOH, the volume of permeable voids (VPV) was determined for the mould cast and printed specimen as shown in Fig. 13. As one could notice in Fig. 13, the mixes with NaOH additive showed higher VPV than the mix with nano clay regardless of the fabrication method (mould cast or 3D printed). Moreover, the difference between the VPV of the mould cast and printed specimen for the mixes with NaOH was insignificant. For instance, the VPV of the mould cast and printed specimens were determined as 10.9% and 11.2% respectively for the mix containing 2.5 wt% NaOH. Similarly, for 5 wt% NaOH content, the corresponding VPV was determined as 12.0% and 12.4% respectively. Therefore, it can be inferred that the low interlayer bond strength of the mixes with NaOH is primarily due to the high porosity of the hardened concrete, compared to M − P mix. This is most likely due to the rapid formation of early age ettringite and the presence of residual PCM in encapsulated-NaOH incorporated mixes causing the increased porosity of the matrix, which in turn reduced the interlayer bond strength in addition to the compressive strength.

Interestingly, the M − P mix with nano clay additive showed a large difference between mould cast and printed specimens compared to NaOH additive mixes. The VPV of printed specimens was 31.1% higher than the mould cast specimens for M − P mix, whereas for the mixes with NaOH, the increment was insignificant (less than 5% increment). While excessive hardening of the printed layer in NaOH incorporated mixes increases the porosity at the interlayer due to cold joints, M − P mix with low-yield strength has poor interlocking between the layers due to extensive deformation while stacking [48]. Moreover, the rapid SYS development of the NaOH incorporated mixes reduces the moisture loss which in turn reduces the formation of pores. The yield strength evolution rate of M − P mix is comparably low, thus showing a higher moisture loss than the NaOH activated mixes. Hence, the increment in VPV from mould cast specimen to printed specimen was higher for the mix containing nano clay (low setting rate mix) than the mixes with NaOH (fast setting rate mix).

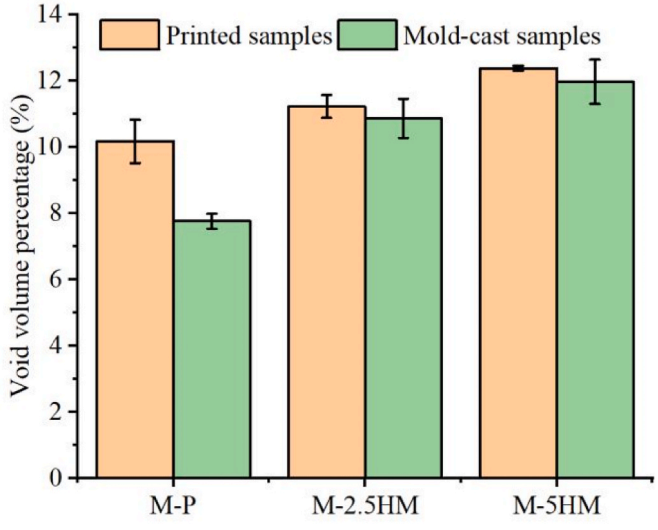

Fig. 13. Volume of permeable voids of printed and mould cast specimens prepared using the mix containing NaOH at various dosages and nano clay (error bar represents mean ± one standard deviation).

5. Feasibility analysis and future studies

The feasibility of proposed stimuli-responsive technique in the context of 3D printing will be assessed by conducting large-scale 3D printing using laboratory 3D printers. For this purpose, a modular print head with the heating system is fabricated as shown in Fig. 14. The printhead is heated by a circulating hot-water system surrounding the extruder. We have investigated different heating mediums including heated coils, electric heating pads, radiant heating system and hot water system. Among these different heating methods, the hot water system provided a regular, uniform and uninterrupted heating supply to the concrete which is essential for uniformly increasing the fresh concrete's temperature. The length of the extruder exposed to the hot water chamber is critical to ensure the adequate heat supply to the concrete to activate the NaOH capsules. This is determined by the residence time of concrete as per the flow rate during the printing. The current prototype uses an approximately 480 mm length extruder exposed to the hot water chamber to raise the concrete's temperature to 35 °C. If the flow rate of concrete is increased, the extruder should be further extended to achieve the targeted temperature rise in concrete. Another concern with this design is that the continuous heat extraction from hot water to fresh concrete and heat loss to the environment will lead to the temperature drop of water in the chamber. Therefore, the hot water is continuously re-circulated by running through a modular water bath using a pump. The designed prototype will be used to print large-scale 3D printed structures with the proposed NaOH capsule based stimuli-response technique. Our future study will assess the proof of concept by evaluating the buildability enhancement and hardened properties of 3D printed structures with this technique.

6. Conclusion

This study investigated a stimuli-responsive method to attain set-on-demand concrete by encapsulating NaOH followed by thermal activation to enhance the buildability in concrete 3D printing. The NaOH at various dosages (0–5 wt% of cement) was encapsulated using a phase change material (PCM) and blended with the cementitious mix during the initial mixing stage. The pre-blended mix was heated at the print head to attain the on-demand setting of the printed layer. The effect of the proposed set-on-demand approach on the fresh and hardened properties of the printable mixes was studied and compared with a traditional buildability enhancement approach by adding a thixotropic additive (nano-clay) during the initial mixing stage. The following are main conclusions drawn from this study:

1. The 3D printable mixes with encapsulated NaOH additive showed excellent pumpability properties before print head thermal activation with an initial slump flow of 185 mm and 165 mm for a dosage of 2.5 wt% and 5 wt% respectively. However, the printable mix containing the nano-clay additive showed zero slump just after the mixing, suggesting poor pumpability properties.
2. The static yield strength (SYS) results showed that simultaneous print head heating and mixing are required to attain significant enhancement in the buildability for the proposed set-on-demand approach. For instance, the mix with 5 wt% of NaOH with printhead heating and mixing showed a SYS of 159.5 kPa at 25 min compared to 34.2 kPa for printhead heating process only.
3. The rate of SYS evolution is much higher than the elastic modulus development for NaOH activation method. The mix with 5 wt% NaOH exhibited SYS growth by % from 10 min to 20 min, whereas the elastic modulus only grew by 24.8% at 20 min.
4. The mechanical properties of compressive strength and interlayer bond strength of 3D printed specimens reveal that the incorporation of encapsulated NaOH reduces both strength properties at 7 and 28 days. Meanwhile, the mix with nano-clay exhibited improved hardened properties than the mix with encapsulated NaOH.

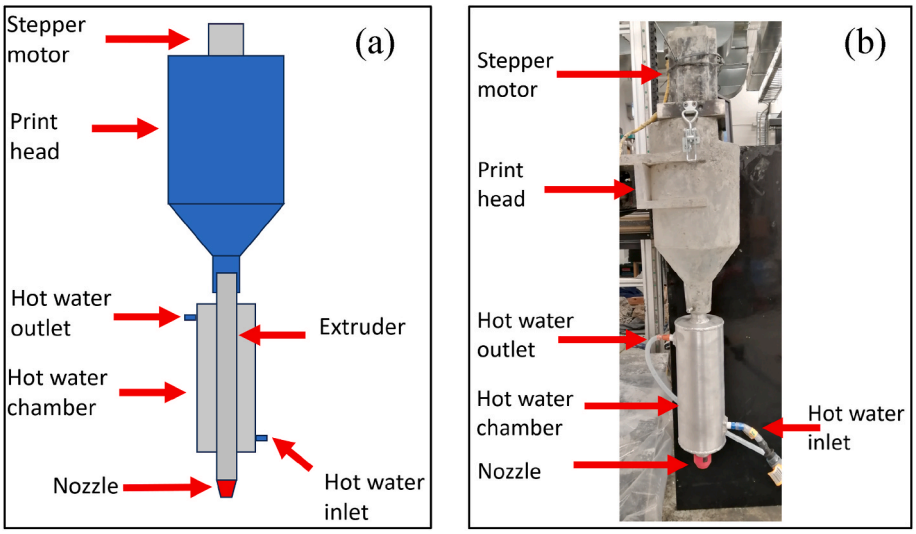

Fig. 14. Prototype of the printhead heating system (a) schematic diagram (b) fabricated prototype.

5. The mixes with encapsulated NaOH showed a high apparent volume of permeable voids (AVPV) for 3D printed and mould cast specimens. The high porosity is due to the formation of secondary ettringite as a result of NaOH and residual PCM in the cement matrix, which has led to the reduced mechanical properties of concrete.

Declaration of competing interest

The authors declare that they have no known competing financial interests or personal relationships that could have appeared to influence the work reported in this paper.

Data availability

Data will be made available on request.

Acknowledgement

The Authors would like to thank the Australian Research Council (ARC) for the financial support provided through the grants of LE170100168 and DE190100646 to conduct the research reported in this paper.

References

[1] G. De Schutter, et al., Vision of 3D printing with concrete — technical, economic and environmental potentials, Cement Concr. Res. 112 (2018) 25–36.
[2] V. Mechtcherine, et al., Extrusion-based additive manufacturing with cement-based materials – production steps, processes, and their underlying physics: a review, Cement Concr. Res. 132 (2020), 106037.
[3] S. Muthukrishnan, S. Ramakrishnan, J. Sanjayan, Technologies for improving buildability in 3D concrete printing, Cement Concr. Compos. (2021), 104144.
[4] B. Panda, J.H. Lim, M.J. Tan, Mechanical properties and deformation behaviour of early age concrete in the context of digital construction, Compos. B Eng. 165 (2019) 563–571.
[5] S. Muthukrishnan, et al., Fresh properties of cementitious materials containing rice husk ash for construction 3D printing, J. Mater. Civ. Eng. 32 (8) (2020), 04020195.
[6] M.A. Moeini, M. Hosseinpoor, A. Yahia, 3D printing of cement-based materials with adapted buildability, Construct. Build. Mater. 337 (2022), 127614.
[7] S. Bhattacherjee, M. Santhanam, Investigation on the effect of alkali-free aluminium sulfate based accelerator on the fresh properties of 3D printable concrete, Cement Concr. Compos. 130 (2022), 104521.
[8] S. Ramakrishnan, S. Kanagasuntharam, J. Sanjayan, In-line activation of cementitious materials for 3D concrete printing, Cement Concr. Compos. (2022), 104598.
[9] Y. Tao, et al., Stiffening control of cement-based materials using accelerators in inline mixing processes: possibilities and challenges, Cement Concr. Compos. (2021), 103972.
[10] J. Huang, et al., On-demand setting of extrusion-based 3D printing gypsum using a heat-induced accelerator, Construct. Build. Mater. 304 (2021), 124624.
[11] F. Boscaro, et al., Eco-Friendly, Set-On-Demand Digital Concrete, 3D Printing and Additive Manufacturing, 2021.
[12] S. Muthukrishnan, S. Ramakrishnan, J. Sanjayan, Effect of microwave heating on interlayer bonding and buildability of geopolymer 3D concrete printing, Construct. Build. Mater. 265 (2020), 120786.
[13] T. Marchment, J. Sanjayan, M. Xia, Method of enhancing interlayer bond strength in construction scale 3D printing with mortar by effective bond area amplification, Mater. Des. 169 (2019), 107684.
[14] N. Makul, et al., Microwave-assisted heating of cementitious materials: relative dielectric properties, mechanical property, and experimental and numerical heat transfer characteristics, Int. Commun. Heat Mass Tran. 37 (8) (2010) 1096–1105.
[15] L. Shao, et al., A novel method for improving the printability of cement-based materials: controlling the releasing of capsules containing chemical admixtures, Cement Concr. Compos. 128 (2022), 104456.
[16] R.S. Langer, D.L. Wise, Medical Applications of Controlled Release, CRC Press LLC, 2019.
[17] J.M. Lakkis, Encapsulation and Controlled Release Technologies in Food Systems, John Wiley & Sons, 2016.
[18] M. Hunger, et al., The behavior of self-compacting concrete containing micro-encapsulated phase change materials, Cement Concr. Compos. 31 (10) (2009) 731–743.
[19] J.L. Reyez-Araiza, et al., Thermal energy storage by the encapsulation of phase change materials in building elements—a review, Materials 14 (6) (2021) 1420.
[20] C. Xue, et al., A review study on encapsulation-based self-healing for cementitious materials, Struct. Concr. 20 (1) (2019) 198–212.
[21] Y.C. Choi, et al., Development and application of microcapsule for cement hydration control, KSCE J. Civ. Eng. 20 (1) (2016) 282–292.
[22] T. Takeuchi, et al., The study on the hydration generation of heat control of the cement by the retarder inclusion microcapsule, Japan Cement Assoc. Proc. Cement Concrete 60 (3) (2007) 568–574.
[23] N. Makul, P. Rattanadecho, D.K. Agrawal, Applications of microwave energy in cement and concrete–a review, Renew. Sustain. Energy Rev. 37 (2014) 715–733.
[24] A. Standards, General Purpose and Blended Cements, 2010.
[25] S. Muthukrishnan, S. Ramakrishnan, J. Sanjayan, Effect of alkali reactions on the rheology of one-part 3D printable geopolymer concrete, Cement Concr. Compos. 116 (2021), 103899.
[26] D. Lootens, et al., Yield stress during setting of cement pastes from penetration tests, Cement Concr. Res. 39 (5) (2009) 401–408.
[27] S. Muthukrishnan, S. Ramakrishnan, J. Sanjayan, In-line activation of geopolymer slurry for concrete 3D printing, Cement Concr. Res. 162 (2022), 107008.
[28] S. Muthukrishnan, S. Ramakrishnan, J. Sanjayan, Set on demand geopolymer using print head mixing for 3D concrete printing, Cement Concr. Compos. 128 (2022), 104451.
[29] ASTM, C1437-07 Standard Test Method for Flow of Hydraulic Cement Mortar. 04.01: p. 2.
[30] C. Liu, et al., Anisotropic mechanical properties of extrusion-based 3D printed layered concrete, J. Mater. Sci. 56 (30) (2021) 16851–16864.
[31] J. Xiao, H. Liu, T. Ding, Finite element analysis on the anisotropic behavior of 3D printed concrete under compression and flexure, Addit. Manuf. 39 (2021), 101712.
[32] D.H. Murcia, M. Genedy, M.R. Taha, Examining the significance of infill printing pattern on the anisotropy of 3D printed concrete, Construct. Build. Mater. 262 (2020), 120559.
[33] O.B. Shalby, et al., Assessment of mechanical and fire resistance for hybrid nano-clay and steel fibres concrete at different curing ages, J. Struct. Fire Eng. 11 (2019) 189–203.

[34] M.K. Mohan, et al., Evaluating the influence of aggregate content on pumpability of 3D printable concrete, in: RILEM International Conference on Concrete and Digital Fabrication, Springer, 2020.
[35] Y. Liu, et al., Effects of aggregate content on rheological properties of lubrication layer and pumping concrete, ACI Mater. J. 118 (6) (2021).
[36] R. Wolfs, F. Bos, T. Salet, Early age mechanical behaviour of 3D printed concrete: numerical modelling and experimental testing, Cement Concr. Res. 106 (2018) 103–116.
[37] R.K. Breitenbücher, Zwangsspannungen und Rissbildung infolge Hydratationswärme, 1989 na.
[38] W.-C. Wang, Compressive strength and thermal conductivity of concrete with nanoclay under Various High-Temperatures, Construct. Build. Mater. 147 (2017) 305–311.
[39] A. Quennoz, K.L. Scrivener, Interactions between alite and C3A-gypsum hydrations in model cements, Cement Concr. Res. 44 (2013) 46–54.
[40] P. Gu, et al., Early strength development and hydration of ordinary Portland cement/calcium aluminate cement pastes, Adv. Cement Base Mater. 6 (2) (1997) 53–58.
[41] S. Ramakrishnan, et al., A novel paraffin/expanded perlite composite phase change material for prevention of PCM leakage in cementitious composites, Appl. Energy 157 (2015) 85–94.
[42] D.P. Bentz, R. Turpin, Potential applications of phase change materials in concrete technology, Cement Concr. Compos. 29 (7) (2007) 527–532.
[43] M. Xia, B. Nematollahi, J. Sanjayan, Printability, accuracy and strength of geopolymer made using powder-based 3D printing for construction applications, Autom. ConStruct. 101 (2019) 179–189.
[44] H. Liu, et al., Influence of pore defects on the hardened properties of 3D printed concrete with coarse aggregate, Addit. Manuf. 55 (2022), 102843.
[45] S. Ramakrishnan, et al., Concrete 3D printing of lightweight elements using hollow-core extrusion of filaments, Cement Concr. Compos. (2021), 104220.
[46] M. van den Heever, et al., Evaluating the effects of porosity on the mechanical properties of extrusion-based 3D printed concrete, Cement Concr. Res. 153 (2022), 106695.
[47] G. Ma, et al., A novel additive mortar leveraging internal curing for enhancing interlayer bonding of cementitious composite for 3D printing, Construct. Build. Mater. 244 (2020), 118305.
[48] I. Dressler, N. Freund, D. Lowke, The effect of accelerator dosage on fresh concrete properties and on interlayer strength in shotcrete 3D printing, Materials 13 (2) (2020) 374.